Chemistry Europe

AWARD

Nominate a Worthy Chemist Chemistry Europe Award

Subject:
chemistry for sustainability, energy, materials, environment

Consists of:
prize money amounting to EUR 10,000, certificate

Deadline:
November 1, 2022

Click here for more info & nomination

ChemPlusChem

Research Article
doi.org/10.1002/cplu.202200224

Chemistry Europe
European Chemical Societies Publishing

www.chempluschem.org

Perfect Polar Alignment of Parallel Beloamphiphile Monolayers: Synthesis, Characterization, and Crystal Architectures of Unsymmetrical Phenoxy-Substituted Acetophenone Azines

Harmeet Bhoday,[a] Michael Lewis,[b] Steven P. Kelley,[b] and Rainer Glaser*[a]

It remains a great challenge to achieve polar order in organic molecular crystals because anti-parallel alignment of side-by-side molecules is intrinsically preferred. We have addressed this problem with a rational design that focuses on the polar stacking of parallel beloamphiphile monolayers (PBAMs) with strong lateral quadrupole-quadrupole attractions. We employ arene-arene interactions as lateral synthons. The first successes were achieved with unsymmetrical donor (X), acceptor (Y) substituted acetophenone azines which form polar PBAMs with double T-contacts between the azines. Near-perfect alignment was achieved with the methoxy series of (MeO, Y)-azines with Y = Cl, Br, I. Here, we report on the synthesis, the characterization (GC/MS, ^{1}H NMR, ^{13}C NMR, FTIR), the crystallization, and the single-crystal X-ray analyses of the phenoxy series of (PhO, Y)-acetophenone azines with Y = F, Cl, Br, I. Properties of (RO, Y) azines were computed at the APFD/6-311G* level and are discussed with reference to *p*-nitroaniline (PNA). This (PhO, Y) series embodies an improved PBAM design based on triple T-contacts which is shown to facilitate faster crystallization and to produce larger crystals. Perfect polar-alignment has been achieved for the phenoxy series of (PhO, Y)-azines with Y = Cl, Br, I and the (PhO, F)-azine also features near-perfect dipole alignment.

Introduction

Advanced material applications that rely on ferroelectricity, second-order non-linear optics (NLO), terahertz wave generation and the electrooptic effect require macroscopic polarity. The design strategies to produce organic crystals with large first-order hyperpolarizabilities have been well documented.[1–3] Polar materials commonly are made by embedding molecular NLO chromophores[4] in polymers and their alignment by electric field poling.[5] Halogen bonding was observed to enhance the NLO response in some poled supramolecular polymers.[6] In a few cases it was possible to grow polar crystals over self-assembled monolayers.[7] Spontaneous dipole alignment in molecular crystals was reported in a few instances: first in 1-galactosamide,[8] later in 4,4′-disubstituted biphenyls discovered by three groups,[9–11] and most recently in the organometallic complex ZNDA.[12] It is important to note that all these dipole parallel-aligned crystalline materials were prepared by different groups and did not lead to general approaches. We have been working on the development of general approaches to achieve polar alignment in crystals of azine materials[13–15] and of oligopeptides[16] by rational design.

To exhibit second-order NLO activity materials must meet the minimal requirement of non-centrosymmetry.[17] Enhanced NLO activity requires the presence of a large macroscopic dipole moment, and this criterion requires orientation of the molecules in the same direction.[14]. Highly polar molecules intrinsically prefer parallel alignment of head-to-tail molecules which are either strictly colinear or may show some lateral offset and anti-parallel alignment of side-by-side molecules as shown in Scheme 1(a) and Scheme 1(b). This arrangement in Scheme 1(a) is centrosymmetric and results in complete dipole cancellation. If centrosymmetry is avoided, the most commonly resulting scenario is depicted in Scheme 1(b) and dipole cancellation is not complete. The ideal polar situation is shown in Scheme 1(c): perfect dipole parallel alignment (DPA) between side-by-side molecules and between head-to-tail molecules. Scheme 1(d) shows a near-perfect scenario for dipole alignment with perfect DPA between side-by-side molecules but only near-perfect DPA between head-to-tail molecules.

The dipole parallel alignment problem presents a striking challenge, and it was thought for a long time that the intrinsic dipole-dipole repulsions associated with parallel alignment cannot be overcome. However, we showed that parallel aligned dipole lattices may occur as local minima.[18] If one were to succeed to stabilize these local minima, then dipole parallel alignment would become achievable by rational design. We make use of lateral intermolecular interactions within the layers to realize large scale polar order in the azine crystals.[19]

We focus on polar conjugated donor-acceptor para-substituted acetophenone azines of the type X–Ar–C(Me) =

[a] H. Bhoday, Prof. R. Glaser
Department of Chemistry
Missouri University of Science and Technology
Rolla, MO 65409 (USA)
E-mail: glaserr@umsystem.edu
[b] Dr. M. Lewis, Dr. S. P. Kelley
Department of Chemistry
University of Missouri
Columbia, MO 65211 (USA)

Supporting information for this article is available on the WWW under https://doi.org/10.1002/cplu.202200224

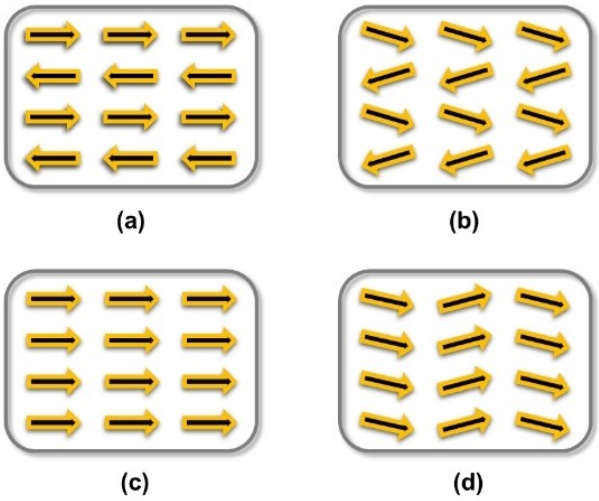

Scheme 1. Dipole-alignment in 2-D: (a) anti-parallel alignment and centro-symmetry, (b) anti-parallel alignment without centrosymmetry, (c) perfect parallel-alignment, and (d) parallel-alignment with a kink.

N–N=C(Me)–Ar–Y with donor X = RO (R = Me, Ph) and acceptor Y = F, Cl, Br, I. Initial success was achieved with the methoxy series of (MeO, Y)-azines over the course of several years.[15]. Here, we report the improved design and realization of a series of ferroelectric crystals of the phenoxy series of (PhO, Y)-azines. Performance data of free chromophores are computed at the APFD/6-311G* level and discussed with reference to *p*-nitroaniline (PNA).[20]

Results and Discussion

Our design of donor-acceptor substituted π-conjugated azines is shown in Scheme 2.[14,15] The first key concept of our design is the minimization of the molecular dipole moment (μ_m). Only molecules with small dipole moments have any chance for dipole parallel alignment. The central azine moiety consists of two polar acceptor imines (AI) with opposite orientations and serves to minimize μ_m by shortening the conjugation length. The long X–Y system of 1,4-diphenylbutadiene is converted into a short X–A(IM) system and one A(IM)–Y system in the azine. This concept works well, and we will show that the dipole moments for the (PhO, Y)-azines are less than half the dipole moment of PNA (7.21 D). To overcome the intrinsic intermolecular dipole-dipole repulsion between side-by-side molecules we employ quadrupole-quadrupole (Q–Q) attraction as our second design concept. We introduce aromatic systems as "lateral synthons", i.e., moieties that provide attractive interactions between side-by-side molecules within an amphiphile monolayer.[19] The intermolecular arene-arene interactions can compensate for the electronic repulsions arising from the dipole parallel alignment. If Q–Q interactions between equally substituted arenes (Q_X–Q_X, Q_Y–Q_Y) exceed Q–Q interactions between oppositely substituted arenes (Q_X–Q_Y), then the overall interaction is maximized for parallel alignment. The azine spacer group not only minimizes the dipole moment but also causes the molecule to adapt a twisted geometry which allows for arene-arene T-type interactions.

Polar alignment in three dimensions was achieved for three representatives of the methoxy series of (MeO, Y)-azines with Y = Cl, Br, I.[21–23] Each (MeO, Y)-azine forms parallel beloamphiphile monolayer (PBAM), that is, parallel

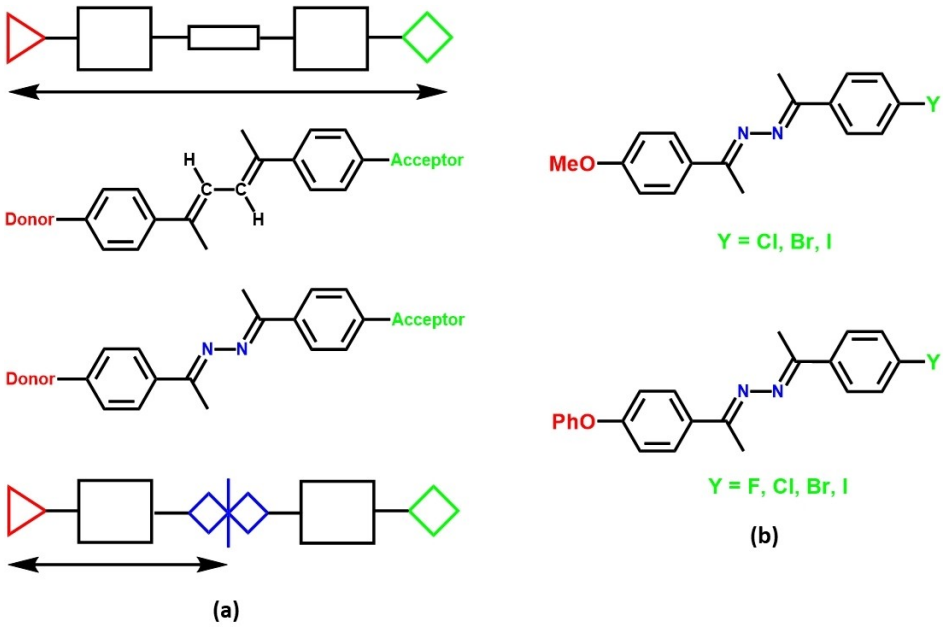

Scheme 2. (a) BAM design to achieve polar stacking of parallel beloamphiphile monolayers (PBAMs). The long X–Y system of the 1,4-diphenylbutadiene is converted into a short X–A(IM) system and one A(IM)-Y system in the azine. (b) Representative molecular structures of the (MeO, Y)- and (PhO, Y)-azines discussed in the paper.

alignment of neighbouring azine molecules in both directions of the layer as shown in Figure 1. The PBAMs of the methoxy series feature lateral offset such that the long axes of the molecules are not perpendicular to the PBAM surface. This offset may be caused by intralayer and/or interlayer interactions (*vide infra*). The leaning angle λ is enclosed between the long axis of each molecule and the normal vector of the layer surface, and the direction of the long axis is defined by the azine N atoms.

The dipole parallel alignment of alkoxy azines in PBAMs is due to intralayer arene-arene C–H···π interactions and specifically arene-arene T-contacts (Scheme 3). A T-contact may involve one C–H bond pointing toward the center of an arene face (^{1}T).[24] A second type of T-contact (^{2}T), and the one relevant in our work, involves an arene edge (e) of the C–H donor to be positioned over the face (f) of the other arene.[25] Such a ^{2}T contact may involve one C–H bond or two C–H bonds of the arene edge to engage in C–H···π interactions. Polar azines engage always in ^{2}T-contacts and we simply refer to them as T-contacts for brevity. Side-by-side pairs of (MeO, Y)-azines interact with two T-contacts, and we refer to this situation as a double T-contact of the type (ef|fe), where one azine acts as (e|f) synthon and the other as (f|e) synthon. The optimization of these double T-contacts may be one source of the observed PBAM offset.

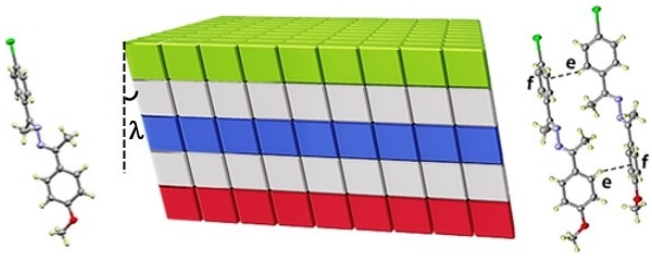

Figure 1. Schematic presentation of a parallel beloamphiphile monolayer (PBAM) of the (MeO, Y) series; green: halogen, grey: arene, blue: azine, red: methoxy. The azine on the left shows the azine twist. The pair shown on the right exemplifies the (ef|fe) double T-contact for (MeO, Cl)-azine.

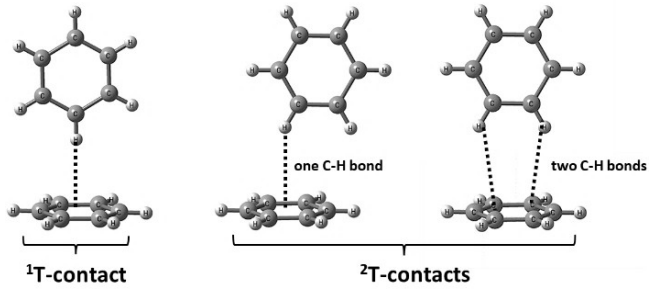

Scheme 3. Arene-arene T-contact types: ^{1}T-contact and ^{2}T-contact. ^{2}T-contacts may be realized with offset (one C–H bond) or without offset (two C–H bonds).

It is expected that polar PBAMs stack in a polar fashion in the third dimension for electrostatic reasons, and this is the case for the PBAMs of the (MeO, Y)-azines (Figure 2).[21–23] It was found that the azines lean in opposite directions in alternating PBAMs and the resulting zigzag stacking pattern is characterized by the kink angle κ and it is caused by directional halogen bonding. The halogen atoms (Cl, Br, I) on the PBAM surface can engage in attractive interactions with the O atoms of the MeO groups on the PBAM surface of the next layer. This is illustrated in Figure 3 for the (MeO, I)-azine layer interface. The PBAMs in all three methoxy azines prefer to stack in a zigzag fashion to maximize the halogen bonding interactions.

The analysis of the interlayer bonding suggested that perfect dipole alignment could be achieved by deliberate avoidance of such halogen bonding interactions. This goal could be met by the replacement of the MeO group by the PhO group. The employment of the larger phenoxy group removes the O atoms substantially from the halogen atoms and clearly avoids interlayer halogen bonding between PBAMs. Moreover, the design of the (PhO, X)-azines offered the additional benefit of triple T-contact formation. This additional, third arene-arene T-contact would increase the lateral interactions and improve the PBAM stability. Hence, we synthesized the phenoxy series of the (PhO, Y)-azines with Y = F, Cl, Br, I.

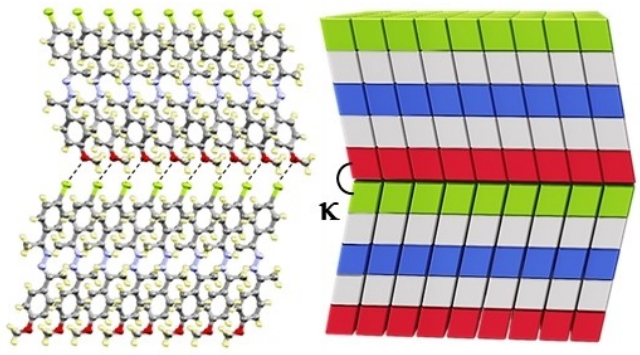

Figure 2. Near-perfect parallel stacking of PBAMs in crystals of (MeO, I)-acetophenone azine due to the directionality of interlayer halogen bonding; note the zigzag pattern. The leaning angles λ are 25.65° (Cl), 25.83° (Br), and 26.02° (I). The kink angles κ are 128.7° (Cl), 128.34° (Br), and 127.96° (I).

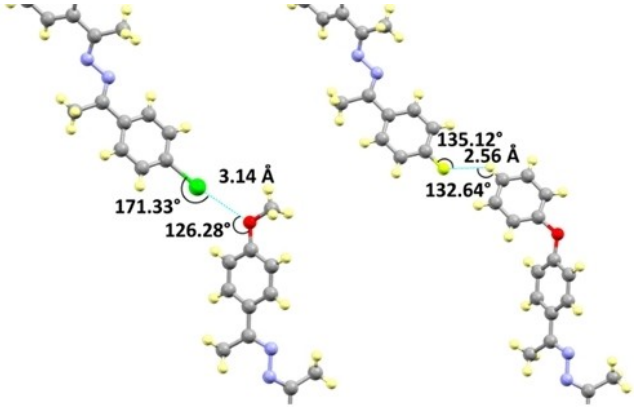

Figure 3. Interlayer interaction between (RO, Y)-azines. Strong directed halogen bonding in (MeO, I)-azine (left). Weak C–H···F interaction in (PhO, F)-azine (right).

Table 1. Computed dipole moments and first-order hyperpolarizabilities of (PhO, Y)- and (MeO, Y)-azines.

Azine	μ_m [a]	β_o [b]	μ_m/V_{vdW} [c]	β_o/V_{vdW} [d]
(PhO, F)	2.7779	15.045	7.9878	43.261
(PhO, Cl)	3.3609	18.509	9.4166	51.859
(PhO, Br)	3.3343	17.978	9.2367	49.803
(PhO, I)	3.4377	18.737	9.3676	51.058
(MeO, F)	2.8952	15.269	10.6506	56.170
(MeO, Cl)	3.5252	18.441	12.5462	65.631
(MeO, Br)	3.4856	18.053	12.2280	63.333
(MeO, I)	3.5960	19.166	12.3555	65.853
PNA	7.2152	10.632	61.0919	90.022

[a] in Debye. [b] in x 10^{-3} Debye Å^{-3}. [c] in x 10^{-3} Debye Å^{-3}. [d] in x 10^{-33} esu Å^{-3}.

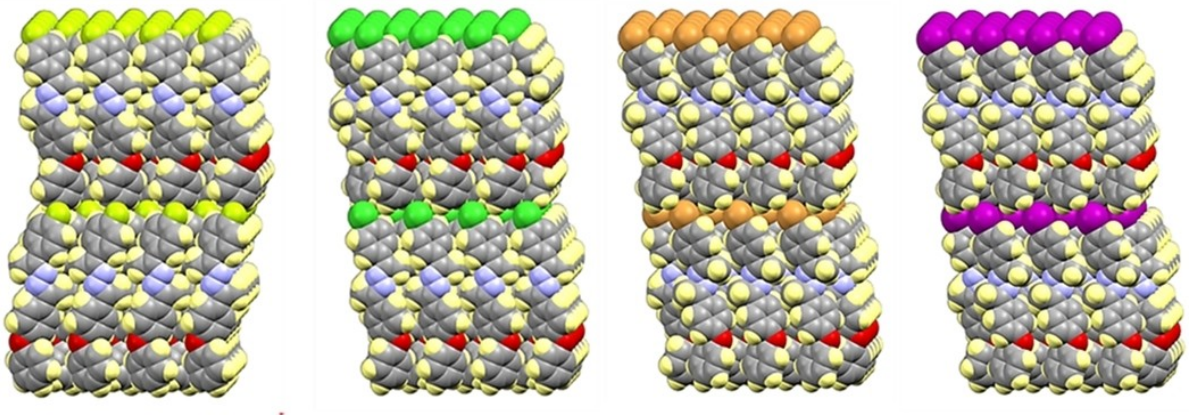

Figure 4. Space-filling bilayer presentations show dipole parallel alignment in crystals of (PhO, Y)-acetophenone azines, from left: Y = F, Cl, Br, I. Near-perfect parallel stacking occurs in crystals of (PhO, F)-acetophenone azine (note the zigzag pattern), but the other halogens afford perfect parallel stacking. The leaning angles are λ(F) = 25.8°, λ(Cl) = 26.27°, λ(Br) = 27.17°, and λ(I) = 26.81°. The kink angles are κ(F) = 128.4° and κ(Y) = 180° for Y = Cl, Br, I.

The synthesis involved coupling of phenoxy-substituted acetophenone with hydrazine hydrate to yield the hydrazone intermediate, which was then condensed with a halogen-substituted acetophenone to yield the desired unsymmetrical (PhO, Y)-azines along with the symmetrical (PhO, PhO)- and (Y, Y)-azines. The azines were separated via column chromatography and the pure products were characterized by mass spectrometry, ^{1}H- and ^{13}C-NMR spectroscopy, and FTIR spectroscopy. Single crystals were grown using slow evaporation techniques. Details of synthesis, characterization, and crystallization are described below. We have published the crystal structures of the symmetrical (PhO, PhO)-azine and of the (PhO, Y)-azines with Y = Cl, Br, I and most recently Y = F. Performance data were computed at the APFD/6-311G* level and in supporting information the complete results are provided for each (PhO, Y)- and (MeO, Y)-azine including dipole moment μ_m, molecular volume V_m, hyperpolarizability tensor elements β_{ijk}, first-order molecular hyperpolarizability β_o, and intensive parameters μ_m/V_m and β_o/V_m. The most pertinent data are summarized in Table 1 and will be discussed in comparison to p-nitroaniline (PNA).

The crystal structures of the four (PhO, Y)-azines with Y = F, Cl, Br, and I are shown in Figure 4, and all exhibit perfect dipole parallel alignment within their PBAMs and polar PBAM stacking. The intralayer arene-arene triple T-contacts are exemplified by one pair in Figure 5. The twists about the N–N bonds and the

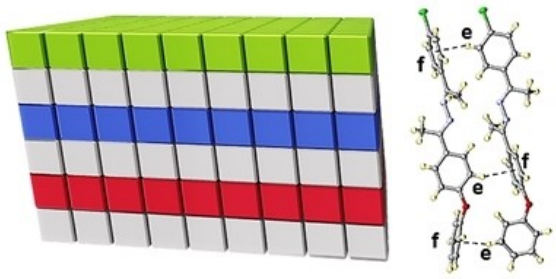

Figure 5. Schematic presentation of a PBAM of the (PhO, Y) series with the same colors as in Figure 1. The MeO- and PhO-series differ substantially in that the oxygen atoms in the latter are well covered by the additional phenyl groups. The pair shown on the right exemplifies the triple T-contact for (PhO, Cl)-azine.

conformation of the diphenyl ether moiety enable each azine to act as (f|e|f) or (e|f|e) synthon in the two PBAM directions and allow the formation pairs of (fe|ef|fe) and (ef|fe|ef) triple T-contacts.

Figure 6 schematically illustrates PBAM stacking types in the phenoxy azines. Replacement of the MeO group by the PhO group avoided any zigzag stacking pattern of PBAMs in the phenoxy azines with Y = Cl, Br, I (Figure 4) and thereby assured perfect dipole parallel alignment as intended by the design. The MeO/PhO replacement also provides an advantage for the

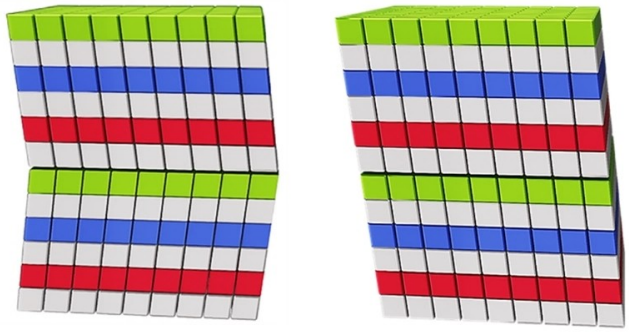

Figure 6. PBAM layer stacking types in (PhO, Y)-acetophenone azines. Near-perfect parallel stacking of PBAMs (left) occurs in crystals of (PhO, F)-azine, while perfect parallel stacking (right) is realized by the (PhO, Y)-azines with all the other halogens Y = Cl, Br, I.

fluoro azine in that (PhO, F)-azine does form polar crystals whereas we have not been able to grow crystals of the (MeO, F)-azine. However, the polar stacking in this case occurs with a kink of $\kappa = 128.4°$. The zigzag pattern in the MeO azines was caused by halogen bonding (Figure 3, left) and there clearly is no possibility for O→F halogen bonding in the PhO-azine. Hence, there must be another directional interaction and analysis of the crystal structure of (PhO, F)-azine indicates that C–H···F interactions cause the kink alignment (Figure 3, right). These kinds of weak C–H···F interactions are well precedented.[26]

The molecular dipole moments μ_m and the first order hyperpolarizabilities β_o are similar for the MeO- and PhO-series of azines (Table 1). The larger space requirement of the phenyl group results in an increase of 26.9 ± 0.7 % of the van der Waals volumes V_{vdW} and decreases of μ_m/V_{vdW} and β_o/V_{vdW} by 24.6 ± 0.3 % and 21.9 ± 0.8 %, respectively. The small reduction in performance is compensated by the much-improved facility to grow single crystals. Even the phenoxy azines still feature β_o/V_{vdW} values of 50 % or more relative to the industry standard PNA. Of course, the reduction of the *molecular* property is more than compensated by the dipole parallel alignment of the azines in their crystals while PNA crystallizes with centrosymmetry.[27] Among the polar aligned azines, the perfect polar stacking of the (PhO, Y)-azines provides an increase of the total crystal dipole moments of about 10 % relative to the near-perfectly aligned (MeO, Y)-azines.

Conclusion

After analyzing the crystal structures of methoxy azines, we modified the design of the polar beloamphiphile monolayer (PBAM) concept to include more arene-arene contacts and to avoid interlayer halogen bonding interactions. Our improved design led to the realization of three perfectly dipole parallel-aligned crystals of (PhO, Y)-azines with Y = Cl, Br, I and one near-perfectly dipole parallel aligned crystal for Y = F. The phenoxy group proved to be a much better donor substituent for perfect dipole parallel alignment in crystals than the methoxy group. The prevalence of the triple T-contact in the crystal structures supports our assertion that a large part of the energy required to overcome the electrostatic repulsion associated with the side-by-side dipole parallel alignment is provided by the strong lateral attractions due to the arene-arene triple T-contacts. Optimization of interlayer interactions to avoid the occurrence of short intermolecular donor-acceptor contacts increased the crystal stability. Ongoing research in our laboratory aims to build on this rational design to prepare stable parallel-aligned organic molecular crystals with improved optical properties and crystallization behavior.

Experimental Section

Synthetic procedure and characterization

The synthesis of the (PhO, Y)-azines is outlined in Scheme S1 of supplementary information. For the synthesis of each (PhO, Y)-azine, 4-phenoxyacetophenone (0.01 mol, 2.12 g) was mixed with 64 % hydrazine monohydrate (0.8 ml) and refluxed in ethanol (20 ml) (2–3 drops of glacial acetic acid were added) to yield more than 95 % of the 4-phenoxyacetophenone hydrazone. The formation of hydrazone completed within 10 hours and the progress of the reaction was monitored by thin-layer chromatography (TLC) using n-hexane and ethyl acetate in the ratio 95 : 5 as solvents. Once the reaction was complete, crystallization of the hydrazone from ethanol helped to remove impurities. The pure crystallized hydrazone was stored dry and sealed to prevent any hydrolysis back to the 4-phenoxyacetophenone. The next step was the condensation reaction of 4-phenoxyacetophenone hydrazone with the halogen-substituted acetophenone supplied in equimolar amounts at reflux in ethanol (2–3 drops of glacial acetic acid were added). The progress of the reaction was monitored by TLC again using n-hexane and ethyl acetate in the ratio 95 : 5 as solvents. The disappearance of the reactant spots on the TLC indicated the completion of the reaction, which was usually achieved after about 24 hours. The reaction produces a mixture of an unsymmetrical (PhO, Y)-azine and the two symmetrical (PhO, PhO)- and (Y, Y)-azines. The desired unsymmetrical (PhO, Y)-azine was the middle spot when the mixture was analyzed by TLC. The separation of (PhO, Y)-azine was accomplished on a silica gel column using n-hexane and ethyl acetate as eluents in the ratio 95 : 5. The desired product was yellow and 4–5 ml fractions were collected in test tubes after the yellow-colored bands started eluting. Around 50 fractions were collected, and TLC was set up for each of the fraction collected. The fraction which only displayed the middle spot was regarded as containing the pure unsymmetrical azine product. This fraction was vacuum dried, and the solid product obtained was characterized by ^{1}H-NMR, ^{13}C-NMR, GC/MS, and FTIR analyses. After characterization, crystals of the phenoxy series of (PhO, Y)-azines were grown using the solvent evaporation technique at room temperature. Crystals with typical widths of 0.2–0.3 mm were grown successfully within 2–3 days. Ethanol and toluene were used as crystallization solvents. For Y = Cl, Br and I, polar crystals were grown in ethanol; for Y = F, toluene turned out to be a better solvent than ethanol. GC/MS data are collected in Table S1, ^{1}H- and ^{13}C-NMR data are collected in Table S2 and Table S3, and characteristic IR frequencies are compiled in Table S4.

Flash Column Chromatography

Analytical thin-layer chromatography was performed on precoated silica gel plates. Visualization of the developed chromatograms was performed by UV absorbance at a wavelength of $\lambda = 254$ nm. For the purification of the substrates, column chromatography using silica gel (particle size 40–63 μm) was performed, using technical grade solvents.

Gas Chromatography/Mass Spectrometry (GC/MS)

GC/MS measurements were conducted on a Shimadzu QP2020 GCMS at the Shared Instrument Laboratory (SIL) of the Department of Chemistry at Missouri University of Science and Technology. The GC peaks are given in min. and the MS peaks are given in m/z units. The methods used for the analyses are shown below in Table S7 and Table S8 and GC/MS spectra of the pure compounds are shown in Figures S1–S4.

Nuclear Magnetic Resonance (NMR) Spectroscopy

^{1}H- and ^{13}C-NMR spectra were acquired on a Bruker instrument at the NMR facility of the Department of Chemistry at Missouri University of Science and Technology. ^{1}H- and ^{13}C-NMR spectra were acquired at 400 MHz and 100 MHz, respectively. The proton signal for the residual non-deuterated solvent (δ 7.24 ppm for $CDCl_3$) was used as an internal reference for ^{1}H-NMR spectra. For ^{13}C-NMR spectra, chemical shifts are reported relative to the δ 77 ppm resonance of $CDCl_3$. ^{1}H-NMR spectra of the four pure (PhO, Y)-azines were recorded at 400 MHz and are shown in Figures S5–S8. Proton-decoupled ^{13}C-NMR spectra of the four pure (PhO, Y)-azines were recorded at 400 MHz and are shown in Figures S9–S12.

Fourier-Transform Infra-Red Spectroscopy (FTIR)

The FTIR spectra for the (PhO, Y)-azines were recorded using ATR-FTIR spectrometer Nicolet iS50 Thermo Scientific in the SIL equipped with a single bounce diamond crystal and a deuterated triglycine sulfate detector. FTIR spectra of the four pure (PhO, Y)-azines are shown in Figures S13–S16.

DFT Calculations of Molecular Dipole Moments and Hyperpolarizability Tensors

(PhO, Y)-, (MeO, Y)-azines and p-nitroaniline (PNA) were studied with density functional theory (DFT) at the APFD/6-311G* level, that is, we employed the Austin-Frisch-Petersson functional with dispersion (APFD) together with the 6–311G* basis set. Table S5 lists the energies, thermochemical data, and molecular properties and Table S6 lists the first order hyperpolarizabilities of p-nitroaniline (PNA), (PhO, Y)- and (MeO, Y)-azines. The optimized structures are shown in Figure S17, and the Cartesian coordinates are provided in Tables S9–S17.

[The following CCDC codes contain the supplementary crystallographic data for this paper. (MeO, Y)-azines with Y = Cl, Br, I: ZIFBUL, CODRES, SUXZAM; (PhO, PhO)-azine: KIGBAK; (PhO, Y)-azines with Y = Cl: NUVPUS, 100 K; Y = Br: KUSNEU, 100 K; KUSNIY, 298 K; Y = I: NUVPOM, 173 K; NUVPIG, 298 K; and Y = F: OBELIU, 150 K. These data can be obtained free of charge from The Cambridge Crystallographic Data Centre via www.ccdc.cam.ac.uk/data_request/cif.]

Acknowledgements

This work was supported by Missouri University of Science and Technology.

Conflict of Interest

The authors declare no conflict of interest.

Data Availability Statement

The data that support the findings of this study are available in the supplementary material of this article.

Keywords: azines · crystal engineering · dipole parallel alignment · ferroelectric crystals · noncovalent interactions

[1] S. J. Kim, B. J. Kang, U. Puc, W. T. Kim, M. Jazbinsek, F. Rotermund, O. P. Kwon, *Adv. Opt. Mater.* **2021**, *9*, 2101019.
[2] S. C. Lee, B. J. Kang, M. J. Koo, S. H. Lee, J. H. Han, J. Y. Choi, W. T. Kim, M. Jazbinsek, H. Yun, D. Kim, F. Rotermund, O. P. Kwon, *Adv. Opt. Mater.* **2017**, *5*, 1600758.
[3] J. H. Seok, D. Kim, W. T. Kim, S.-J. Kim, W. Yoon, G.-E. Yoon, I. C. Yu, M. Jazbinsek, S.-W. Kim, H. Yun, D. Kim, F. Rotermund, O. P. Kwon, *Adv. Opt. Mater.* **2021**, *9*, 2100324.
[4] S.-H. Jang, J. Luo, N. M. Tucker, A. Leclercq, E. Zojer, M. A. Haller, T.-D. Kim, J.-W. Kang, K. Firestone, D. Bale, J. Lao, B. Benedict, D. Cohen, W. Kaminsky, B. Kahr, J. L. Brédas, P. Reid, L. R. Dalton, A. K.-Y. Jen, *Chem. Mater.* **2006**, *18*, 2982.
[5] S. Miyata, H. Sasabe, *Poled Polymers and their Applications to SHG and EO Devices*, Gordon and Breach, Amsterdam, **1997**.
[6] M. Virkki, O. Tuominen, A. Forni, M. Saccone, P. Metrangolo, G. Resnati, M. Kauranen, A. Priimagi, *J. Mater. Chem. C* **2015**, *3*, 3003.
[7] R. Hiremath, S. W. Varney, J. A. Swift, *Chem. Mater.* **2004**, *16*, 4948.
[8] M. Masuda, T. Shimizu, *Chem. Commun.* **2001**, 2442.
[9] R. Glaser, N. Knotts, Z. Wu, C. L. Barnes, *Cryst. Growth Des.* **2006**, *6*, 235.
[10] L. Walz, H. Paulus, W. Haase, *Z. Kristallogr.* **1987**, *180*, 97.
[11] J. Zyss, I. Ledoux, M. Bertault, E. Toupet, *Chem. Phys.* **1991**, *150*, 125.
[12] S. P. Anthony, T. P. Radhakrishnan, *Chem. Commun.* **2001**, 931.
[13] S. S. Chourasiya, D. Kathuria, A. A. Wani, P. V. Bharatam, *Org. Biomol. Chem.* **2019**, *17*, 8486.
[14] R. Glaser, N. Knotts, P. Yu, L. Li, M. Chandrasekhar, C. Martin, C. L. Barnes, *Dalton Trans.* **2006**, 2891.
[15] R. Glaser, *Acc. Chem. Res.* **2007**, *40*, 9.
[16] S. Khanra, S. V. Vassiliades, W. A. Alves, K. Yang, R. Glaser, K. Ghosh, P. Bhattacharya, P. Yu, S. Guha, *AIP Adv.* **2019**, *9*, 115202(1).
[17] C. Bosshard, R. Spreiter, U. Meier, I. Liakatas, M. Bösch, M. Jäger, S. Manetta, S. Follonier, P. Günter (Eds.: D. Braga, F. Grepioni), *Organic Materials for Second-Order Nonlinear Optics*, Kluwer, Dordrecht, **1991**, p. 261.
[18] D. Steiger, C. Ahlbrandt, R. Glaser, *J. Phys. Chem. B* **1998**, *102*, 4257.
[19] M. Lewis, Z. Wu, R. Glaser, *ACS Symposium Series, Vol. 798* (Eds.: R. Glaser, P. Kaszynski), American Chemical Society: Washington, D. C., **2001**, 97.
[20] Gaussian 16, Revision C.01, M. J. Frisch, G. W. Trucks, H. B. Schlegel, G. E. Scuseria, M. A. Robb, J. R. Cheeseman, G. Scalmani, V. Barone, G. A. Petersson, H. Nakatsuji, X. Li, M. Caricato, A. V. Marenich, J. Bloino, B. G. Janesko, R. Gomperts, B. Mennucci, H. P. Hratchian, J. V. Ortiz, A. F. Izmaylov, J. L. Sonnenberg, D. Williams-Young, F. Ding, F. Lipparini, F. Egidi, J. Goings, B. Peng, A. Petrone, T. Henderson, D. Ranasinghe, V. G. Zakrzewski, J. Gao, N. Rega, G. Zheng, W. Liang, M. Hada, M. Ehara, K. Toyota, R. Fukuda, J. Hasegawa, M. Ishida, T. Nakajima, Y. Honda, O. Kitao, H. Nakai, T. Vreven, K. Throssell, J. A. Montgomery, Jr., J. E. Peralta, F. Ogliaro, M. J. Bearpark, J. J. Heyd, E. N.

Brothers, K. N. Kudin, V. N. Staroverov, T. A. Keith, R. Kobayashi, J. Normand, K. Raghavachari, A. P. Rendell, J. C. Burant, S. S. Iyengar, J. Tomasi, M. Cossi, J. M. Millam, M. Klene, C. Adamo, R. Cammi, J. W. Ochterski, R. L. Martin, K. Morokuma, O. Farkas, J. B. Foresman, D. J. Fox, Gaussian, Inc., Wallingford CT, **2016**.
[21] G. S. Chen, J. K. Wilbur, C. L. Barnes, R. Glaser, *J. Chem. Soc. Perkin Trans. 2* **1995**, 2311.
[22] M. Lewis, C. Barnes, R. Glaser, *Acta Crystallogr. Sect. C* **2000**, 56, 393.
[23] M. Lewis, C. Barnes, R. Glaser, *J. Chem. Crystallogr.* **2000**, *30*, 489.
[24] E. Arunan, H. S. Gutowsky, *J. Chem. Phys.* **1993**, *98*, 4294.
[25] A. Katrusiak, M. Podsiadzo, A. Budzianowski, *Cryst. Growth Des.* **2010**, *10*, 3461.
[26] V. R. Thalladi, H.-C. Weiss, D. Blaser, R. Boese, A. Nangia, G. R. Desiraju, *J. Am. Chem. Soc.* **1998**, *120*, 8702.
[27] M. Colapietro, A. Domenicano, C. Marciante, G. Portalone, *Z. Naturforsch. B* **1982**, *37*, 1309.

Manuscript received: July 7, 2022
Revised manuscript received: August 30, 2022

RESEARCH ARTICLE

Achieving polar order in organic molecular crystals is a challenging task. This work addresses this problem with a rational design that focuses on the polar stacking of parallel beloamphiphile monolayers (PBAMs) with strong lateral arene-arene interactions. The synthesis, the crystallization, and the properties of the phenoxy series of (PhO, Y)-acetophenone azines with Y = F, Cl, Br, I are reported. This series embodies a PBAM design based on triple T-contacts. Perfect polar-alignment has been achieved for the phenoxy series of (PhO, Y)-azines with Y = Cl, Br, I and the (PhO, F)-azine also features near-perfect dipole alignment.

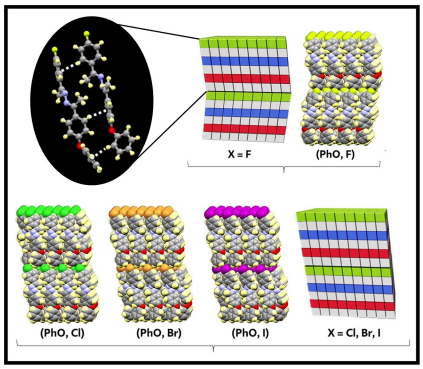

*H. Bhoday, Dr. M. Lewis, Dr. S. P. Kelley, Prof. R. Glaser**